Published in final edited form as:
Int J Cancer. 2011 July 1; 129(1): 233–244. doi:10.1002/ijc.25666.

Increased Efficacy of Doxorubicin Delivered in Multifunctional Microparticles for Mesothelioma Therapy

Jedd M. Hillegass[1,*], **Steven R. Blumen**[1,*], **Kai Cheng**[4,*], **Maximilian B. MacPherson**[1], **Vlada Alexeeva**[1], **Sherrill A. Lathrop**[1], **Stacie L. Beuschel**[1], **Jeremy L. Steinbacher**[4], **Kelly J. Butnor**[1], **Maria E. Ramos-Niño**[1], **Arti Shukla**[1], **Ted A. James**[3], **Daniel J. Weiss**[2], **Douglas J. Taatjes**[1], **Harvey I. Pass**[5], **Michele Carbone**[6], **Christopher C. Landry**[4], and **Brooke T. Mossman**[1]

[1] Department of Pathology, University of Vermont College of Medicine, Burlington, VT

[2] Department of Medicine, University of Vermont College of Medicine, Burlington, VT

[3] Department of Surgery, University of Vermont College of Medicine, Burlington, VT

[4] Department of Chemistry, University of Vermont, Burlington, VT

[5] Department of Cardiothoracic Surgery, NYU School of Medicine, New York, NY

[6] Cancer Research Center of Hawaii, University of Hawaii, Honolulu, HI

Abstract

New and effective treatment strategies are desperately needed for malignant mesothelioma (MM), an aggressive cancer with a poor prognosis. We have shown previously that acid-prepared mesoporous microspheres (APMS) are nontoxic after intrapleural or intraperitoneal (IP) administration to rodents. The purpose here was to evaluate the utility of APMS in delivering chemotherapeutic drugs to human MM cells *in vitro* and in two mouse xenograft models of MM. Uptake and release of doxorubicin (DOX) alone or loaded in APMS (APMS-DOX) were evaluated in MM cells. MM cell death and gene expression linked to DNA damage/repair were also measured *in vitro*. In two SCID mouse xenograft models, mice received saline, APMS, DOX, or APMS-DOX injected directly into subcutaneous (SC) MM tumors or injected IP after development of human MMs peritoneally. Other mice received DOX intravenously (IV) via tail vein injections. In comparison to DOX alone, APMS-DOX enhanced intracellular uptake of DOX, MM death, and expression of *GADD34* and *TP73*. In the SC MM model, 3X weekly SC injections of APMS-DOX or DOX alone significantly inhibited tumor volumes, and systemic DOX administration was lethal. In mice developing IP MMs, significant ($p<0.05$) inhibition of mesenteric tumor numbers, weight, and volume was achieved using IP administration of APMS-DOX at one-third the DOX concentration required after IP injections of DOX alone. These results suggest APMS are efficacious for the localized delivery of lower effective DOX concentrations in MM, and represent a novel means of treating intracavitary tumors.

Keywords

Microparticles; Mesoporous silica; Mesothelioma; Doxorubicin; Intracavitary tumors

Corresponding author: Brooke T. Mossman, PhD, University of Vermont College of Medicine, Department of Pathology, 89 Beaumont Avenue, Burlington, VT 05405-0068, USA, F: 802-656-8892, brooke.mossman@uvm.edu.

*Note that the first three authors contributed equally to this research

Novelty

Nanomaterials are being advocated for the delivery of cancer chemotherapeutics, but their systemic distribution to other organs including the brain has raised questions regarding their safety. Malignant mesothelioma (MM) is an aggressive cancer with a poor prognosis despite numerous treatment strategies. To overcome these limitations, we developed nontoxic, micron-sized, acid-prepared mesoporous spheres (APMS) to allow administration of drugs or constructs to intracavitary tumors such as MM. Specifically, we suggest the use of APMS to enhance the local delivery and effectiveness of cancer chemotherapeutics and to avoid systemic toxicity.

Impact

APMS have been engineered in a size range (1–2 μm diameter) that favors tumor cell uptake, yet prohibits entry into the systemic circulation. Studies here show that local administration of APMS preloaded with doxorubicin (DOX) increase sustained delivery of DOX, and inhibit growth of human MM tumors *in vitro* and in immunocompromised SCID mice without evidence of systemic toxicity. In addition to increasing delivery of chemotherapeutics, APMS can be tagged with targeting moieties such as antibodies and modified to introduce DNA/siRNA constructs, thus facilitating multi-targeted therapeutic approaches.

Introduction

New treatment strategies are desperately needed for the intracavitary tumor, malignant mesothelioma (MM), which typically originates from mesothelial cells of the pleura, peritoneum or pericardium. Current therapies for MM include systemic chemotherapy, gene therapy, surgery, radiation, or palliative procedures.[1] The effectiveness of intracavitary chemotherapy is also a topic of intense examination,[2, 3] including the administration of intracavitary hyperthermic chemotherapy.[4, 5] Single modality therapies have little effect on patient survival, while multiple modality therapies are only slightly more effective.[6–11] For example, doxorubicin (DOX), has been utilized in the treatment of a variety of cancers, including MM and breast cancer, but can cause cardiac and systemic toxicity.[12] The ineffectiveness of systemic chemotherapy in treating MM may be due to inefficient delivery and uptake of chemotherapeutics. Thus, to increase cell uptake of DOX and to circumvent its systemic toxicity, we explored the use of a novel system to deliver DOX directly to MM cells via local administration.

Vehicles for loading and delivery of chemotherapeutic drugs or molecular constructs have been featured recently in the cancer literature.[13–15] Although nanomaterials have been advocated for drug delivery to some tumor types, their limitations include penetration and consequent dysfunction of cellular organelles, and the possibility of systemic toxicity due to entrance into the blood stream and transport to other organs.[16, 17] To overcome these limitations and to avoid systemic dissemination, we developed nontoxic, micron-sized particles to allow their injection directly into established tumors, sites of surgical resection of tumors, and peritoneal or thoracic cavities.

Acid-prepared mesoporous spheres (APMS) are porous, amorphous silica microspheres (1–2 μm in diameter) with a pore diameter that is tunable between 40 and 100 Å to allow loading of drugs, functional plasmids,[18] or DNA/siRNA constructs.[19, 20] In contrast to crystalline silicas, amorphous silicas are less durable and are nontoxic.[21] We have shown recently that

APMS functionalized with tetraethylene glycol (TEG) are nontoxic *in vitro* or after intranasal instillation or intrapleural injection into mice, and that this functionalization promotes phagocytosis and uptake by murine lung epithelial and human MM cells *in vitro*.[18] In studies here, we hypothesized that using APMS at sites of MM tumor development might be advantageous as a novel form of localized chemotherapy delivery to avoid systemic toxicity.

We first demonstrated that APMS-TEG loaded with DOX in comparison to DOX alone led to significantly ($p<0.05$) increased delivery and drug uptake by MMs, increased MM cell death *in vitro*, and enhanced expression of genes linked to DNA damage and death (cell cycle arrest and apoptosis) pathways. Next, we performed *in vivo* studies with fluorescently labeled APMS-TEG to confirm particle uptake by subcutaneous (SC) MMs growing in severe combined immunodeficient (SCID) mice, as well as by pleural cells and cells in peritoneal lavage fluid (PLF) after injection of APMS-TEG into the pleural or intraperitoneal (IP) cavities. In the SC human MM xenograft model, we found that localized injection of APMS-TEG loaded with microgram quantities of DOX was more effective in inhibition of SC tumor growth and nontoxic to mice when compared to systemic DOX administration. Lastly, we utilized an IP human MM xenograft model to demonstrate that 3-fold lower concentrations of APMS-TEG-loaded DOX (APMS-DOX) are equally effective in inhibiting IP tumor growth as higher concentrations of DOX alone. Our results suggest that APMS are an effective approach for the localized delivery of chemotherapeutic drugs typically associated with systemic toxicity.

Materials and Methods

Cells and reagents

Human pleural MM cell lines isolated from surgical resection of MMs or at autopsy were kind gifts from Drs. Luciano Mutti (Maugeri Foundation, Pavia, Italy; MO), Maurizio Bocchetta (Loyola University, Mayfair, IL; ME-26) and Harvey Pass (NYU School of Medicine, New York, NY; PPM Mill, PPM Rob, PPM Ada, PPM Gar, PPM Gates, PPM Gord). All isolates were confirmed as MM cells by immunohistochemistry using an antibody to calretinin and verified for lack of mycoplasma contamination using a polymerase chain reaction (PCR) assay prior to use in studies described here. Hmeso cells, originally designated H-MESO-1, were initially isolated by Reale *et al*,[22] and supplied by Drs. Joseph Testa and Deborah Altomare (Fox Chase Cancer Institute, Philadelphia, PA). Cell culture procedures were as described.[18]

Synthesis of APMS-TEG and preloading with doxorubicin (DOX)

Synthesis of APMS and surface modification with TEG have been described previously.[18] Hereafter, APMS-TEG will be referred to simply as APMS. APMS were loaded with DOX via incubation with a saturated aqueous solution of DOX-HCl (Sigma, St. Louis, MO) for 16 h, and then isolated with centrifuge membrane filters (Nanosep MF 0.45 μm, Pall Corporation, Ann Arbor, MI) and dried under vacuum at room temperature in the dark.

Treatment of MM cells with APMS, APMS-DOX, DOX and cisplatin

For initial studies examining differences in DOX delivery via HPLC, the sarcomatoid MM cell line (MO) was plated in complete medium at 37°C. When cells reached 70–80% confluency, the complete medium was aspirated and replaced with maintenance medium (containing 0.5% FBS) for 24 h. APMS were then suspended in maintenance medium at a concentration of approximately 6×10^7 APMS/100 μl, and sonicated 5X for 2 sec to achieve an even suspension. Fifty μl were then added to cells at a final concentration of 7.5×10^6 APMS/cm^2 surface area dish (~185 APMS/cell). DOX (160 nM) was added directly to

maintenance medium and APMS-DOX (160 nM DOX equivalent) was prepared and administered as described above. Cell killing effects of DOX alone, APMS alone, DOX added simultaneously with APMS, and APMS loaded with DOX (APMS-DOX) were assessed using both the MO MM line and an epithelioid MM line (ME26) cultured and treated as described above. Finally, 7 MM cell lines (Hmeso, PPM Mill, PPM Rob, PPM Ada, PPM Gar, PPM Gates, and PPM Gord) were evaluated in dose-response studies to determine their relative sensitivity to DOX and cisplatin. Cells were grown as described above to near confluency, and DOX (0–25 μM) and cisplatin (0–75 μM) were added directly to maintenance medium.

Determination of extracellular and intracellular DOX concentration

After incubation of MO cells with either DOX (160 nM) in medium or APMS-DOX (160 nM DOX equivalent), medium was centrifuged at 10,000 × g at 4°C. The supernatant was then transferred to fresh vials, Daunorubicin (a fluorescent internal standard) added (final concentration of 1 μM), and the vial vortexed prior to incubation at 37°C for 15 min. Proteins were precipitated by adding 250 μl of acetone and 50 μl of aqueous $ZnSO_4$ solution (400 mg/ml) to the sample and vortexing prior to incubation at 37°C for 15 min. Samples were subsequently centrifuged at 20,000 × g (10 min) at 4°C, and supernatants transferred to new vials and dried at room temperature for 2 h under vacuum. The residue was solubilized in 500 μl of MeOH, and a volume of 100 μl used for HPLC analysis. To determine the intracellular DOX concentration, MO cells were trypsinized, centrifuged at 1,000 rpm in cold phosphate-buffered saline (PBS), supernatants removed, and cells resuspended in 190 μl of PBS and 5 μl lysis solution (Triton X-100, 3%). Five μl of proteinase K (10 mg/ml stock solution) then was added. Samples were incubated for 45 min in a water bath at 65°C, and 56.4 μl of 10 μg/ml Daunorubicin was then added to a final volume of 400 μl with PBS. Five μl of phenylmethylsulfonyl fluoride (PMSF) was added for 10 min prior to the addition of 10 μl $MgCl_2$ (0.4 M) and 20 μl DNase I (1 mg/ml). After centrifugation, the sample was incubated in a water bath at 37°C for 30 min, and 450 μl of methanol and 45 μl of $ZnSO_4$ (400 mg/ml) added to 450 μl of each sample. After mixing, the sample was centrifuged for 5 min, and a volume of 100 μl used for HPLC analysis.

High Pressure Liquid Chromatography (HPLC)

A published HPLC method for detection of DOX was modified to allow quantitation of extracellular and intracellular amounts of DOX.[23–25] The HPLC system consisted of a 1525 Binary HPLC Pump, a 717 Plus Autosampler, and a 2475 Multi-Wavelength Fluorescence Detector (Waters Corporation, Milford, CT). Chromatography was performed on a BDS Hypersil C18 column (4×150 mm, particle size 5 μm). The mobile phase consisted of water:acetronitrile:tetrahydrofuran (75.5:24:0.5, v/v/v), with an apparent pH adjusted to 2.0 with perchloric acid. The flow rate was maintained at 1.25 ml/min with an injection volume of 40 μl or 100 μl. The effluents were monitored at an excitation wavelength of 480 nm and an emission wavelength of 560 nm at 40°C. Detection and integration of chromatographic peaks was performed using Breeze Chromatography v.3.20 software.

Lactate dehydrogenase (LDH) assay

Cell lysis was measured by determining levels of LDH in the medium of MO or ME26 cells treated with either APMS (7.5×10^6 APMS/cm^2), varying concentrations of DOX (40–800 nM), or APMS-DOX (7.5×10^6 APMS/cm^2; 10–80 nM DOX equivalent) using a Cytotox 96® Non-Radioactive Cytotoxicity Assay (Promega Corporation, Madison, WI) per the manufacturer's recommendations.[18] The percentage of LDH release was calculated based on complete lysis induced by a positive control lysis buffer (0.09% Triton-X).

MTS assay

MO cell viability following treatment with medium alone, DOX alone (80 nM), APMS (7.5×10^6 APMS/cm^2), or APMS-DOX (7.5×10^6 APMS/cm^2; 80 nM DOX equivalent), was measured *in vitro* using the colorimetric MTS assay, CellTiter 9® AQ_{ueous} One Solution Cell Proliferation Assay (Promega) as per the manufacturer's recommendations.

Preparation of RNA and PCR Array analyses

To determine if different patterns of gene expression related to cellular DNA damage/repair were observed after addition of DOX alone or APMS-DOX, RNA from MO cells treated with medium alone, APMS alone (7.5×10^6 APMS/cm^2), DOX alone (80 nM), or APMS-DOX (7.5×10^6 APMS/cm^2; 80 nM DOX equivalent) for 24 h was prepared and purified using a RNeas® Plus Mini Kit (Qiagen, Valencia, CA). After quality assessment, 1 μg of RNA was employed for cDNA synthesis using the RT^2 First Strand Kit (SABiosciences, Frederick, MD). Quantitative real-time PCR (QRT-PCR) was performed by the Vermont Cancer Center DNA Analysis Facility using RT^2 Real-Time™ SYBR Green PCR Master Mix and Human DNA Damage Signaling Pathway RT^2 Profiler™ PCR Arrays (SABiosciences) (7900HT Sequence Detection System, Applied Biosystems, Foster City, CA). QRT-PCR (TaqMan) was used to validate selected genes using Assay on Demand (AOD) Primers and Probes (Applied Biosystems). For the purposes of these studies, only gene changes ≥3-fold are provided.

Confocal Scanning Laser Microscopy (CSLM) for determination of APMS-Alexa-568 and APMS-Alexa-488 localization *in vivo*

APMS were covalently labeled with the fluorescent dye, Alexa Fluor 568 (APMS-Alexa-568), by standard peptide-bond forming methodology.[18] APMS-Alexa-568 were suspended in PBS at a concentration of approximately 3.3×10^7 APMS/100 μl PBS. C57BL/6 mice (n = 3; Jackson Laboratories, Bar Harbor, ME) received intrapleural injections and were euthanized after 72 h.[18] Rib cage and adjacent diaphragm were removed surgically and either placed in Tissue-Tek O.C.T® compound and snap-frozen, or fixed in 4% paraformaldehyde and paraffin embedded. For determination of tumor uptake, 5×10^6 Hmeso cells were injected into 4 subcutaneous (SC) sites on the dorsa of 6 week old male Fox Chase strain severe combined immunodeficient (SCID) mice (Jackson Laboratories, Bar Harbor, ME). Tumors appearing at 21 days were injected on day 28 at the distal pole of the tumor with 3×10^6 APMS labeled with Alexa Fluor 488 succinimide ester (APMS-Alexa-488) for 24 h and removed for processing and step sectioning. Tissue section slides from frozen tissues were prepared,[18] and representative images were acquired using a Zeiss LSM 510 META confocal scanning laser microscope (Carl Zeiss Microimaging Inc., Thornwood, NY). All animal studies were approved by the Institutional Animal Care and Use Committee at the University of Vermont.

Inhibition of human MM growth in subcutaneous (SC) and intraperitoneal (IP) mouse xenograft models

In the SC xenograft model, Hmeso cells (5×10^6 cells/injection site in 50 μl 0.9% NaCl, pH 7.4, hereafter referred to simply as saline) were injected into 4 sites on the dorsa of 6 week-old male Fox Chase strain SCID mice (Jackson Laboratories) under isoflurane anesthesia. This MM line was selected because of its intermediate sensitivity to DOX and cisplatin *in vitro* (see Results) and its reproducible tumor growth and phenotype (biphasic MM). Tumors were first characterized by a board certified pathologist using previously described criteria[26, 27] to confirm their mesothelial origin. In an initial study (Experiment 1) utilizing the SC model (n = 2 mice or 8 MM tumors/group), Hmeso tumors appearing at 19 days post-injection were injected 1X weekly at their distal poles for 3 weeks with 50 μl saline

alone, APMS (3×10^8 APMS/tumor, equivalent to 160 mg/kg APMS) in saline, DOX (6.15 μg DOX/tumor injection, equivalent to a total concentration of 1 mg/kg DOX/mouse) in saline, or APMS-DOX (3×10^8 APMS; 6.15 μg DOX equivalent/tumor) in saline. Another group of mice received injections of DOX (5 mg/kg) at concentrations known to inhibit MM growth in rats[28] via intravenous (IV) tail vein injection. All mice were weighed weekly and examined every other day for tumor growth and morbidity. When the largest axes of the tumors in the control mice reached 1 cm, mice were euthanized as described above, necropsied to determine possible metastases, and major organs removed and stored in 4% paraformaldehyde before processing for histopathology and evaluation by a board-certified pathologist. Tumors were weighed and were measured using digital calipers. Tumor volumes were calculated using the formula (π × long axis × short axis × short axis)/6. Since the 1X weekly injection regimen failed to inhibit tumor growth, a second experiment was performed (n = 4 mice or 16 MM tumors/group) in which agents were administered 3X weekly (Experiment 2).

In the intraperitoneal (IP) xenograft model (Experiment 3), Hmeso cells (5×10^6 cells in 50 μl saline) were injected into the lower left quadrant of the peritoneal cavity of 6 week-old male Fox Chase strain SCID mice (n = 5 mice/group). After 2 weeks, a time period in which all mice developed non-adherent spheroid MMs (see below), mice were injected IP 3X over the course of 1 week with 500 μl saline alone, DOX (1 mg/kg) in saline, or APMS-DOX (7.8×10^8 APMS/mouse, equivalent to 0.33 mg/kg DOX) in saline. Based on our results in Experiment 2, in which we did not see a difference in tumor growth between APMS-DOX and DOX alone groups when administered SC at a higher concentration (1 mg/kg; see Results), we administered a lower dose of DOX (0.33 mg/kg) in APMS to demonstrate increased efficiency of this delivery method. In addition, this DOX concentration is similar to the dose of DOX delivered during intracavitary MM chemotherapy in humans (15 mg/m^2, equivalent to 0.41 mg/kg).[3] An APMS alone group was not included in Experiment 3 since separate studies have demonstrated that IP doses of APMS up to 500 mg/kg (equivalent to 3.8×10^9 APMS/mouse) are well tolerated in mice (data not shown). Mice were euthanized as described above, and tumors were classified as either “spheroid” (small, free-floating nodules) or larger “mesenteric” tumors attached to the peritoneal mesentery. The total number of spheroid or mesenteric tumors/mouse was determined, along with individual tumor volume and weight. For each mouse, total tumor weight and volume were calculated separately for spheroids and mesenteric tumors by multiplying the average tumor weight and volume by the total number of spheroid and mesenteric tumors present, respectively. A summary of all *in vivo* xenograft studies and treatment regimens is presented in Table 1.

Collection and preparation of peritoneal lavage fluid (PLF) for cytospins

To determine the presence of free APMS and those associated with cells in PLF in Experiment 3, the peritoneal cavity of each mouse was instilled with 5 ml of cold sterile PBS using an 18-gauge needle. Leaving the needle in place, the abdomen was gently massaged and PLF was aspirated back into the syringe and placed on ice. Cytospin slides were generated as described,[18] and representative photographs were taken using an Olympus BX50 microscope (Olympus America Inc., Lake Success, NY) and QCapture Pro v.6.0 software.

Statistical analysis

For all *in vitro* experiments, at least 3 independent experiments were performed (n = 2–4 samples/experiment). For *in vivo* tumor experiments, results are representative of 2–5 mice/group/experiment. Statistical significance was evaluated by ANOVA using the Student Neuman-Keul’s procedure for adjustment of multiple pairwise comparisons between

treatment groups or using the non-parametric Kruskal-Wallis, Mann-Whitney or Tukey HSD tests. Values of $p<0.05$ were considered statistically significant.

Results

We first studied the amounts of DOX delivered to MO cells *in vitro* after administration in medium alone or via APMS-DOX. Since DOX becomes rapidly bound to DNA, use of DNase to release DOX from DNA and subsequent addition of MeOH and $ZnSO_4$ were necessary for accurate quantitation by fluorescence HPLC. Similar methodology was used to quantify the amount of extracellular DOX. Whereas the left axis (Figure 1A and 1B) displays the percentage of the total dose of DOX, the right axis shows the actual dose (ng) of DOX/plate of cells. Since the total amount of DOX contained within APMS prior to their addition to MMs was known, the amount of DOX remaining within the APMS over time could be determined. A small amount (10–15%) of DOX was initially detected in medium, presumably through leakage from APMS after sonication (Figure 1A). Over a 24 h period, intracellular DOX increased until a maximum of approximately 50% of the initial amount within the APMS was released. More importantly, the balance of DOX remained within the APMS for 48 h, allowing further release over time. In contrast, the maximum amount of DOX transferred to cells when DOX was added directly to medium was approximately 25% of the initial dose (Figure 1B). The drop in intracellular DOX concentration observed at 48 h in APMS-DOX treated cultures (Figure 1A) is likely due to decreases in the overall number of cells available for analysis as a result of increased APMS-DOX cell death between 24 and 48 h of exposure.

To comparatively assess the effects of DOX alone, DOX added simultaneously (but separately) with APMS, and APMS-DOX, dose-response studies were first performed on the sarcomatoid MO MM line. Initially, a range of concentrations of DOX were incubated with MO cells for 24 or 48 h, and LDH release into the medium was determined as a measure of lytic cell damage. Little LDH release (<10%) was seen with doses of DOX alone ranging from 40 to 800 nM (Figure 2A; top panel). In contrast, addition of APMS-DOX caused a dose-related release of LDH. At 48 h, approximately 50% of total cell lysis was achieved at 65 nM DOX (Figure 2A; middle panel). This potency was not achieved when individual preparations of APMS and DOX were incubated simultaneously with MO cells (Figure 2A; bottom panel). These data also show that APMS alone at the highest concentrations (7.5×10^6 APMS/cm^2 surface area of dish, equivalent to amounts loaded with 65 nM DOX in the APMS-DOX group) were nontoxic to cells over a 48 h period.

To further verify the more potent toxic effects of APMS-DOX on MM cells, we assessed cell viability using an MTS assay over 96 h (Figure 2B). When MO cells were exposed to either 80 nM DOX or APMS alone (7.5×10^6 APMS/cm^2 surface area of dish, equivalent to amounts loaded with 80 nM DOX), there were no significant differences in cell viability in comparison to untreated cells. However, when cells were treated with APMS-DOX, significant ($p<0.05$) decreases in cell viability occurred at 48 h and thereafter. We next verified the increased potency of APMS-DOX in the LDH assay using ME26 cells (Figure 2C). By 48 h, the APMS-DOX (80 nM DOX equivalent) group showed a significantly ($p<0.05$) higher amount of lytic cell death, i.e., ~20% of total release, in contrast to 80 nM DOX alone. Because the greatest cytotoxic effects of APMS-DOX were achieved in sarcomatoid MMs, which have the worst prognosis,[29] we performed further mechanistic studies on the MO MM line.

To shed light on the mechanisms of DNA damage by DOX and whether these were exacerbated in DOX delivery by APMS, we performed PCR array analysis on genes associated with apoptosis, cell cycle regulation, and various forms of DNA repair. Treatment

of MO cells with DOX (80 nM) or APMS-DOX (80 nM DOX equivalent) caused at least 3-fold ($p<0.05$) increased expression of 6 genes (*GADD45A*, *GADD153*, *GADD34*, *IHPK3*, *BTG2*, *TP73*) in comparison to untreated MO cells (Figure 2D). In contrast, mRNA levels of *GSTE1* were significantly ($p<0.05$) decreased. Messenger RNA levels of RAD50 were increased ($p<0.05$) in response to APMS-DOX (80 nM DOX equivalent), but not DOX alone (80 nM). In addition, *GADD34* and *TP73* gene expression was significantly ($p<0.05$) elevated in response to APMS-DOX when compared to the DOX alone group. No significant gene expression alterations were observed with APMS alone. QRT-PCR was used to confirm significantly ($p<0.05$) increased gene expression of *GADD45A* and *GADD34* in both DOX and APMS-DOX-treated cells (data not shown). These data indicate increased responses to DNA damage after delivery of APMS-DOX versus DOX alone to MM cells.

To determine whether APMS could enter and remain in tissues *in vivo* adjacent to sites of APMS injection, 3.3×10^7 APMS-Alexa-568 were injected into the pleural cavities of C57BL/6 mice (n = 3). Using CSLM, APMS-Alexa-568 were located adjacent to sites of injection in the soft tissue surrounding the ribs (Figure 3A and 3B). As reported previously, [18] APMS-Alexa-568 were seen occasionally in the diaphragm, lung, and spleen using fluorescence microscopy. We then used SCID mice developing MMs after SC injection of Hmeso cells to determine whether APMS-Alexa-488 injected at the distal pole of the tumor migrated to the interior of the tumor. As shown in Figure 3C, APMS-Alexa-488 (green) were detected in the cytoplasm of MM cells in tumor masses. When cytospins were evaluated following IP administration of APMS-DOX (Experiment 3), APMS were detected in PLF samples, indicating these particles remain within the peritoneal cavity up to 10 d (Figure 3D). Further, it appears as if most APMS are associated with MMs and macrophages, although additional studies are required to confirm this observation.

Our final goal was to demonstrate the efficacy of APMS-DOX in a SCID mouse xenograft model. We first tested a number of human MM lines for their sensitivity to DOX or cisplatin over a range of concentrations *in vitro* and for reproducible tumor growth in SCID mice. The maximum concentration of DOX used in these dose-response studies (25 μM) was approximately equal to DOX concentrations achieved in peritoneal fluids (18.4 μM or 10 μg/ml) following intracavitary DOX chemotherapy (15 mg/m^2 or 0.41 mg/kg) in patients with MMs.[3] Dose-response experiments with cisplatin were also performed in each cell line to determine if patterns of drug resistance were the same as DOX in individual MM lines.[4, 30] These studies revealed that different human MMs were heterogeneous in their sensitivity to either DOX or cisplatin (Figure 4A and 4B). Moreover, the patterns of sensitivity to both drugs were similar in individual MMs. Since the Hmeso MM line expressed intermediate sensitivity to drugs in comparison to other MM lines and grew reproducibly after injection into SCID mice, this line was selected for *in vivo* studies.

As shown in Experiment 1 (Figure 4C), 1X weekly SC injections of APMS alone, DOX (1 mg/kg), APMS-DOX (1 mg/kg) or IV administration of DOX (5 mg/kg) over a 3 week period did not affect Hmeso tumor growth (n = 2 mice/group). Although histopathological analysis of organs revealed diffuse hepatocytic ballooning in the livers of mice administered DOX IV, no other adverse events were observed in organs evaluated from other treatment groups. However, when agents were administered 3X weekly (Experiment 2), tumor volume failed to increase after day 40 following SC injections of DOX (1 mg/kg) or APMS-DOX (1 mg/kg), and was significantly ($p<0.05$) lower in these groups in comparison to saline or APMS treated groups at the termination of the experiment (n = 4 mice/group) (Figure 4D). In these experiments, systemic administration of DOX (5 mg/kg) was lethal to all mice after 2 sequential IV doses (data not shown).

In Experiment 3, using an IP xenograft model (n = 5 mice/group), we reduced the concentration of DOX loaded in APMS (0.33 mg/kg) to determine if we could demonstrate increased or equivalent efficacy as DOX alone at 3-fold higher concentrations (1 mg/kg). In comparison to saline controls, mesenteric MM tumor numbers (Figure 5A), volumes (Figure 5B), and weights (Figure 5C) were significantly ($p<0.05$) less in mice administered DOX (1 mg/kg) or APMS-DOX (0.33 mg/kg) IP 3X weekly. Although not statistically significant, it appears administration of DOX and APMS-DOX also decreased growth of spheroid tumors. Hematoxylin and eosin staining of representative spheroid (Figure 5D) and mesenteric (data not shown) tumors indicate a biphasic MM tumor type.

Discussion

Limited effective treatment strategies exist for patients with MM. Many chemotherapeutic drugs, including DOX, have been used in single or combination therapies with most current treatments resulting in a mean survival time of 12–15 mos.[1, 6–11, 31, 32] Most cancer chemotherapeutic drugs cause adverse systemic side effects because of their lack of tumor specificity and necessary administration at high doses. Thus, we hypothesized that using APMS at sites of MM tumor development might be advantageous as a novel form of localized chemotherapy delivery to avoid systemic toxicity. We show here in preclinical studies that APMS are an attractive vehicle to administer chemotherapeutic drugs and to enhance their delivery, cellular uptake, and cytotoxic effects. The APMS surface can be modified to contain a myriad of functional moieties, including fluorescent molecules for detection, gadolinium for MRI tracking (Steinbacher et al., unpublished data; Lathrop et al., unpublished data), and antibodies for targeting specific tumor types (Cheng et al., unpublished data). Functionalizing the exterior surface of APMS with molecules such as TEG enables rapid uptake by target cells by a process evading lysosomal degradation.[18] Other important characteristics of mesoporous microparticles are their large surface areas (up to 1100 m^2/g) and pore volumes (>1.0 cm^3/g) that are advantageous in loading a large amount of 'cargo'.[33–37]

Cisplatin and DOX have proven to be more effective than a variety of single chemotherapeutic drugs in single modality treatment of MM.[1, 6–10] Because DOX is more chemically stable and quantifiable using HPLC it was selected for our studies. In addition to showing increased drug delivery and toxicity of APMS-DOX to MMs *in vitro*, we reveal the increased expression of a number of genes influencing DNA damage/repair. DNA damage is generally regarded as the primary cause of DOX-induced cell death in tumor cells. The molecular events linking DOX-induced DNA signaling to cell death have not been defined, but may involve cell signaling cascades, free radical-mediated events, and DOX-DNA adduct formation.[38, 39] Upregulation of 3 *GADD* (growth arrest and DNA damage response) genes was observed in DOX or APMS-DOX-treated MM cells. Although *GADD45* is an oxidative stress responsive gene induced by DOX in a number of cell types, expression of *GADD153* (DNA-damage-inducible, alpha or *DDIT3*), a redox-activated gene that plays a role in cell cycle arrest, apoptosis, and activation of signal transduction pathways following DNA damage, is a novel finding that may be important in combination chemotherapy of MMs. Increased mRNA expression of *IHPK3* (inositol hexaphosphate kinase 3), a gene linked to the development of apoptosis, and *BTG2* (BTG family member 2), a less well-characterized p53-mediated DNA damage response gene associated with DNA repair, were also increased by DOX or APMS-DOX administration in our studies. Moreover, G*ADD34* and *TP73* mRNAs were increased ($p<0.05$) more dramatically in MM cells after exposure to APMS-DOX in comparison to DOX alone, presumably because of the increased delivery of DOX when loaded into APMS. The increased expression of *TP73* (encoding Tumor protein p73) in MMs treated with APMS-DOX was another novel observation in our gene array studies. This gene has been previously implicated in regulating a p53-dependent apoptotic

pathway in tumors treated with chemotherapeutic drugs.[40] In contrast to the well-studied *p53* gene that encodes a tumor suppressor gene mediating cell cycle arrest or apoptosis in response to DNA damage, the *TP73* gene encodes an array of isoforms not possessing typical tumor suppressor gene functions (reviewed in[41, 42]).

Significant ($p<0.05$) decreases in *GTSE-1* expression, which encodes a cell cycle-regulated protein (hGSTE-1 or human $G_{(2)}$ and S-phase expressed-1), were also observed in both DOX and APMS-DOX treated MM cells. Since hGSTE-1 is able to down-regulate p53 levels and activity,[43] its decreased expression in drug-treated MM cells may represent a repair mechanism whereby p53 function is kept intact.

Overall, studies have demonstrated that APMS are a novel and effective tool for enhanced delivery of DOX. Localized administration of APMS-DOX inhibits tumor cell growth in mouse models of MM via SC or IP injection in the absence of systemic toxicity. Most importantly, 3-fold lower effective concentrations of DOX were achieved after loading in APMS as opposed to injection of DOX alone in an IP mouse xenograft model of MM. In this model, APMS-DOX or DOX was injected when all of the mice had pre-established MM spheroids as demonstrated in preliminary experiments. Although DOX has been incorporated into RGD-modified[44] and polyethylene glycol-derivatized liposomes[45] and nanoparticles[46] to increase its stability in the intravascular compartment, our studies are unique in that APMS were engineered in a size range (1–2 μm diameter) favoring tumor cell uptake (via TEG functionalization) at sites of local and intracavitary injection and prohibiting entrance into the systemic circulation, a major problem in DOX-associated cardiotoxicity.[47] Infusion of APMS-DOX or other chemotherapeutic drugs into the pleural or peritoneal cavity could potentially inhibit the growth of premalignant MM cells in pleural/peritoneal fluids. Additionally, the ability to functionalize drug-loaded APMS with targeting moieties such as anti-mesothelin antibodies (Cheng et al., unpublished data), and the ability of APMS to release DNA[20] and introduce functional plasmids into tumor cells,[18] are exciting approaches that could potentially result in more effective treatment regimens for MMs and other cancers.

Acknowledgments

We thank Jennifer Díaz and Trisha Barrett for technical assistance with this manuscript, and Drs. Sean McCarthy and Albert van der Vliet (Department of Pathology, UVM) for help with HPLC analyses. Dr. Pamela Vacek (Department of Medical Biostatistics, UVM) was valuable in performing statistical analyses. We also appreciate the technical assistance of the Vermont Cancer Center DNA Facility staff with PCR Array and QRT-PCR analyses. This work was supported by the Mesothelioma Applied Research Foundation (MARF to BTM), a Small Business Technology Transfer (STTR) grant from the National Cancer Institute (R41 CA126155 to CCL), and a training grant from the National Institute of Environmental Health Sciences (T32 ES007122 to JMH).

Abbreviations used

APMS	Acid-prepared mesoporous spheres
MM	Malignant mesothelioma
DOX	Doxorubicin
IP	Intraperitoneal
APMS-DOX	Doxorubicin loaded APMS
SC	Subcutaneous
IV	Intravenous
TEG	Tetraethylene glycol

SCID	Severe combined immunodeficient
PCR	Polymerase chain reaction
MO	Sarcomatoid MM cell line
PMSF	Phenylmethylsulfonyl fluoride
HPLC	High Pressure Liquid Chromatography
LDH	Lactate dehydrogenase
QRT-PCR	Quantitative real-time PCR
AOD	Assay on Demand
PLF	Peritoneal lavage fluid
ME26	Epithelioid MM cells

References

1. Vogelzang NJ. Emerging insights into the biology and therapy of malignant mesothelioma. Semin Oncol. 2002; 29:35–42. [PubMed: 12571809]
2. Hesdorffer ME, Chabot JA, Keohan ML, Fountain K, Talbot S, Gabay M, Valentin C, Lee SM, Taub RN. Combined resection, intraperitoneal chemotherapy, and whole abdominal radiation for the treatment of malignant peritoneal mesothelioma. Am J Clin Oncol. 2008; 31:49–54. [PubMed: 18376228]
3. Van der Speeten K, Stuart OA, Mahteme H, Sugarbaker PH. A pharmacologic analysis of intraoperative intracavitary cancer chemotherapy with doxorubicin. Cancer Chemother Pharmacol. 2009; 63:799–805. [PubMed: 18654746]
4. Richards WG, Zellos L, Bueno R, Jaklitsch MT, Janne PA, Chirieac LR, Yeap BY, Dekkers RJ, Hartigan PM, Capalbo L, Sugarbaker DJ. Phase I to II study of pleurectomy/decortication and intraoperative intracavitary hyperthermic cisplatin lavage for mesothelioma. J Clin Oncol. 2006; 24:1561–7. [PubMed: 16575008]
5. van Ruth S, van Tellingen O, Korse CM, Verwaal VJ, Zoetmulder FA. Pharmacokinetics of doxorubicin and cisplatin used in intraoperative hyperthermic intrathoracic chemotherapy after cytoreductive surgery for malignant pleural mesothelioma and pleural thymoma. Anticancer Drugs. 2003; 14:57–65. [PubMed: 12544259]
6. Pass, H.; Carbone, M.; Vogelzang, N. Malignant mesothelioma: advances in pathogenesis, diagnosis, and translational therapies. New York: Springer Science+Business Media, Inc; 2005. p. 854
7. Sterman DH, Albelda SM. Advances in the diagnosis, evaluation, and management of malignant pleural mesothelioma. Respirology. 2005; 10:266–83. [PubMed: 15955137]
8. Grondin SC, Sugarbaker DJ. Pleuropneumonectomy in the treatment of malignant pleural mesothelioma. Chest. 1999; 116:450S–4S. [PubMed: 10619506]
9. Krug LM. An overview of chemotherapy for mesothelioma. Hematol Oncol Clin North Am. 2005; 19:1117–36. vii. [PubMed: 16325127]
10. Tomek S, Emri S, Krejcy K, Manegold C. Chemotherapy for malignant pleural mesothelioma: past results and recent developments. Br J Cancer. 2003; 88:167–74. [PubMed: 12610498]
11. Mukohara T, Civiello G, Johnson BE, Janne PA. Therapeutic targeting of multiple signaling pathways in malignant pleural mesothelioma. Oncology. 2005; 68:500–10. [PubMed: 16020981]
12. Steele, JPC.; Rudd, RM. Systemic chemotherapy for malignant pleural mesothelioma. In: O'Byrne, K.; Rusch, V., editors. Malignant Pleural Mesothelioma. Oxford: Oxford University Press; 2006. p. 297-313.
13. Bartlett DW, Su H, Hildebrandt IJ, Weber WA, Davis ME. Impact of tumor-specific targeting on the biodistribution and efficacy of siRNA nanoparticles measured by multimodality in vivo imaging. Proc Natl Acad Sci U S A. 2007; 104:15549–54. [PubMed: 17875985]

14. Feazell RP, Nakayama-Ratchford N, Dai H, Lippard SJ. Soluble single-walled carbon nanotubes as longboat delivery systems for platinum(IV) anticancer drug design. J Am Chem Soc. 2007; 129:8438–9. [PubMed: 17569542]
15. Liu Z, Chen K, Davis C, Sherlock S, Cao Q, Chen X, Dai H. Drug delivery with carbon nanotubes for in vivo cancer treatment. Cancer Res. 2008; 68:6652–60. [PubMed: 18701489]
16. Pantarotto D, Briand JP, Prato M, Bianco A. Translocation of bioactive peptides across cell membranes by carbon nanotubes. Chem Commun (Camb). 2004:16–7. [PubMed: 14737310]
17. Oberdorster G, Maynard A, Donaldson K, Castranova V, Fitzpatrick J, Ausman K, Carter J, Karn B, Kreyling W, Lai D, Olin S, Monteiro-Riviere N, et al. Principles for characterizing the potential human health effects from exposure to nanomaterials: elements of a screening strategy. Part Fibre Toxicol. 2005; 2:8. [PubMed: 16209704]
18. Blumen SR, Cheng K, Ramos-Nino ME, Taatjes DJ, Weiss DJ, Landry CC, Mossman BT. Unique uptake of acid-prepared mesoporous spheres by lung epithelial and mesothelioma cells. Am J Respir Cell Mol Biol. 2007; 36:333–42. [PubMed: 17038662]
19. Gallis, KW.; Landry, CC. Mesoporous silica and method of making same United States. 2002.
20. Solberg SM, Landry CC. Adsorption of DNA into mesoporous silica. J Phys Chem B. 2006; 110:15261–8. [PubMed: 16884243]
21. Guthrie, GD., Jr; Mossman, BT. Health Effects of Mineral Dustsed. 28. Washington, DC: Mineralogical Society of America; 1993. p. 584
22. Reale FR, Griffin TW, Compton JM, Graham S, Townes PL, Bogden A. Characterization of a human malignant mesothelioma cell line (H-MESO-1): a biphasic solid and ascitic tumor model. Cancer Res. 1987; 47:3199–205. [PubMed: 3555770]
23. de Bruijn P, Verweij J, Loos WJ, Kolker HJ, Planting AS, Nooter K, Stoter G, Sparreboom A. Determination of doxorubicin and doxorubicinol in plasma of cancer patients by high-performance liquid chromatography. Anal Biochem. 1999; 266:216–21. [PubMed: 9888978]
24. Burden DA, Osheroff N. Mechanism of action of eukaryotic topoisomerase II and drugs targeted to the enzyme. Biochim Biophys Acta. 1998; 1400:139–54. [PubMed: 9748545]
25. Swift LP, Rephaeli A, Nudelman A, Phillips DR, Cutts SM. Doxorubicin-DNA adducts induce a non-topoisomerase II-mediated form of cell death. Cancer Res. 2006; 66:4863–71. [PubMed: 16651442]
26. Rdzanek M, Fresco R, Pass HI, Carbone M. Spindle cell tumors of the pleura: differential diagnosis. Semin Diagn Pathol. 2006; 23:44–55. [PubMed: 17044195]
27. Martarelli D, Catalano A, Procopio A, Orecchia S, Libener R, Santoni G. Characterization of human malignant mesothelioma cell lines orthotopically implanted in the pleural cavity of immunodeficient mice for their ability to grow and form metastasis. BMC Cancer. 2006; 6:130. [PubMed: 16704740]
28. Linden CJ. Response to doxorubicin and cyclophosphamide of a human pleural mesothelioma clinically and as a xenograft in nude rats. In Vivo. 1990; 4:55–9. [PubMed: 2103842]
29. Kobayashi M, Takeuchi T, Ohtsuki Y. Establishment of three novel human malignant pleural mesothelioma cell lines: morphological and cytogenetical studies and EGFR mutation status. Anticancer Res. 2008; 28:197–208. [PubMed: 18383846]
30. Matsuzaki Y, Tomita M, Shimizu T, Hara M, Ayabe T, Onitsuka T. Induction of apoptosis by intrapleural perfusion hyperthermo-chemotherapy for malignant pleural mesothelioma. Ann Thorac Cardiovasc Surg. 2008; 14:161–5. [PubMed: 18577894]
31. Mossman BT, Gee JB. Asbestos-related diseases. N Engl J Med. 1989; 320:1721–30. [PubMed: 2659987]
32. Robinson BW, Lake RA. Advances in malignant mesothelioma. N Engl J Med. 2005; 353:1591–603. [PubMed: 16221782]
33. Beck J, Vartuli J, Roth W, Leonowicz M, Kresge C, Schmitt K, Chu C, Olson D, Sheppard E. A new family of mesoporous molecular sieves prepared with liquid crystal templates. J Am Chem Soc. 1992; 114:10834–43.
34. Kresge C, Leonowicz M, Roth W, Vartuli J, Beck J. Ordered mesoporous molecular sieves synthesized by a liquid-crystal template mechanism. Nature. 1992; 359:710–2.

35. Slowing II, Vivero-Escoto JL, Wu CW, Lin VS. Mesoporous silica nanoparticles as controlled release drug delivery and gene transfection carriers. Adv Drug Deliv Rev. 2008; 60:1278–88. [PubMed: 18514969]
36. Vallet-Regi M, Balas F, Arcos D. Mesoporous materials for drug delivery. Angew Chem Int Ed Engl. 2007; 46:7548–58. [PubMed: 17854012]
37. Vinu A, Hossain KZ, Ariga K. Recent advances in functionalization of mesoporous silica. J Nanosci Nanotechnol. 2005; 5:347–71. [PubMed: 15913241]
38. Huang X, Halicka HD, Traganos F, Tanaka T, Kurose A, Darzynkiewicz Z. Cytometric assessment of DNA damage in relation to cell cycle phase and apoptosis. Cell Prolif. 2005; 38:223–43. [PubMed: 16098182]
39. Zhao Y, You H, Yang Y, Wei L, Zhang X, Yao L, Fan D, Yu Q. Distinctive regulation and function of PI 3K/Akt and MAPKs in doxorubicin-induced apoptosis of human lung adenocarcinoma cells. J Cell Biochem. 2004; 91:621–32. [PubMed: 14755690]
40. Sabatino MA, Previdi S, Broggini M. In vivo evaluation of the role of DNp73alpha protein in regulating the p53-dependent apoptotic pathway after treatment with cytotoxic drugs. Int J Cancer. 2007; 120:506–13. [PubMed: 17096333]
41. Benard J, Douc-Rasy S, Ahomadegbe JC. TP53 family members and human cancers. Hum Mutat. 2003; 21:182–91. [PubMed: 12619104]
42. Stiewe T, Putzer BM. Role of p73 in malignancy: tumor suppressor or oncogene? Cell Death Differ. 2002; 9:237–45. [PubMed: 11859406]
43. Monte M, Benetti R, Collavin L, Marchionni L, Del Sal G, Schneider C. hGTSE-1 expression stimulates cytoplasmic localization of p53. J Biol Chem. 2004; 279:11744–52. [PubMed: 14707141]
44. Xiong XB, Huang Y, Lu WL, Zhang X, Zhang H, Nagai T, Zhang Q. Intracellular delivery of doxorubicin with RGD-modified sterically stabilized liposomes for an improved antitumor efficacy: in vitro and in vivo. J Pharm Sci. 2005; 94:1782–93. [PubMed: 15986461]
45. Gabizon AA, Barenholz Y, Bialer M. Prolongation of the circulation time of doxorubicin encapsulated in liposomes containing a polyethylene glycol-derivatized phospholipid: pharmacokinetic studies in rodents and dogs. Pharm Res. 1993; 10:703–8. [PubMed: 8321835]
46. Barraud L, Merle P, Soma E, Lefrancois L, Guerret S, Chevallier M, Dubernet C, Couvreur P, Trepo C, Vitvitski L. Increase of doxorubicin sensitivity by doxorubicin-loading into nanoparticles for hepatocellular carcinoma cells in vitro and in vivo. J Hepatol. 2005; 42:736–43. [PubMed: 15826724]
47. Lu P. Monitoring cardiac function in patients receiving doxorubicin. Semin Nucl Med. 2005; 35:197–201. [PubMed: 16098293]

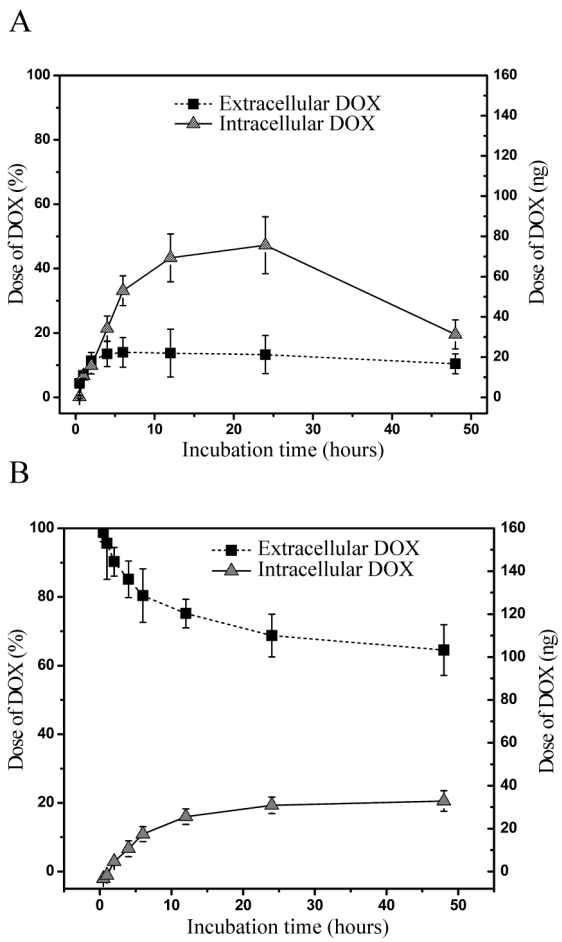

Figure 1.

Determination of DOX uptake *in vitro* via HPLC following two different methods of administration to sarcomatoid (MO) MM cells for up to 48 h. Extracellular and intracellular DOX levels in MO cells measured by HPLC show greater cell delivery and retention of DOX when (**A**) loaded and released from APMS (APMS-DOX; 7.5×10^6 APMS/cm^2; 160 nM DOX equivalent) in comparison to (**B**) direct addition to medium (160 nM DOX). Points represent the mean ± SEM (n = 3 in triplicate experiments).

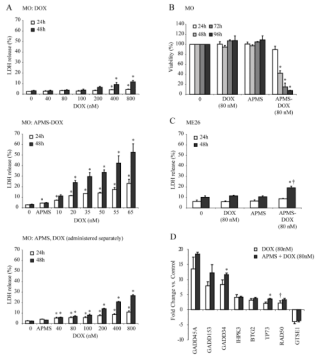

Figure 2.

APMS-DOX delivery increases cytotoxicity in both sarcomatoid (MO) and epithelioid (ME26) MM cells *in vitro*. Cell lysis and viability were determined using the LDH and MTS assays, respectively. (**A**) LDH release by MO cells was measured under several treatment conditions including exposure to DOX alone (40–800 nM; top panel), exposure to APMS preloaded with varying concentrations of DOX (7.5×10^6 APMS/cm^2, 10–65 nM DOX equivalent; middle panel), and exposure to individual preparations of unloaded APMS (7.5×10^6 APMS/cm^2) and DOX (40–800 nM) simultaneously (bottom panel). (**B**) MTS viability assay confirming increased cytotoxicity of APMS-DOX (7.5×10^6 APMS/cm^2; 80 nM DOX equivalent) in MO cells. (**C**) LDH release by ME26 cells. For LDH, percent release was calculated based on a complete lysis induced by a positive control lysis buffer (0.09% Triton-X; data not shown). For (A, B, C), 0 = medium only control; bars represent the mean ± SEM of n = 2–4 treatment groups in duplicate or more experiments; * = $p<0.05$ in comparison to medium alone at same time point; † = $p<0.05$ in comparison to DOX alone group. (**D**) PCR array experiments reveal alteration in several genes related to DNA damage and repair in sarcomatoid (MO) MM cells treated with DOX (80 nM) or APMS-DOX (7.5×10^6 APMS/cm^2; 80 nM DOX equivalent) for 24 h. Upregulation of 6 genes and downregulation of 1 gene was observed following treatment with DOX or APMS-DOX compared to cells treated with medium alone. No significant gene expression alterations were observed with APMS alone. Only gene changes ≥3-fold are provided. * = $p<0.05$ in comparison to DOX alone group. † = not significant compared to medium control group. Bars represent the mean +/− SEM of n = 3 plates/group.

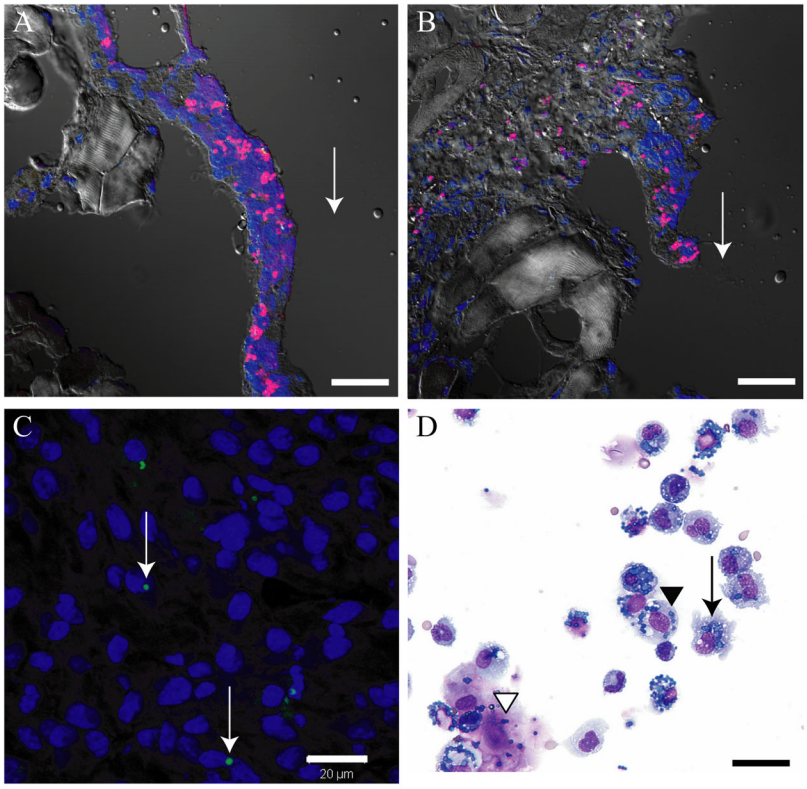

Figure 3.

Several *in vivo* experiments demonstrate that APMS are taken up by a variety of cell types and remain adjacent to sites of injection. (**A, B**) APMS-Alexa-568 (red) injected into the pleural cavity of C57BL/6 mice were found in cells lining the rib at 72 h post-injection. Cell nuclei are stained blue (TOTO-3). Arrows indicate the approximate site of APMS injections. Approximately 3.3×10^7 APMS-Alexa-568 were injected into individual mice (× 400, scale bars = 20 μm). (**C**) APMS-Alexa-488 (green) injected at the distal pole of Hmeso SC tumors grown in SCID mice were detected within the cytoplasm of individual MM cells towards the center of the tumor mass. Tumor cell nuclei are stained blue (DAPI). Arrows indicate the presence of APMS-Alexa-488 signal. Approximately 3×10^6 APMS-Alexa-488 were injected into individual tumors (× 400, scale bar = 20 μm). (**D**) Representative PLF cytospin showing co-localization of APMS with macrophages (arrow), sloughed mesothelial cells (black arrowhead), and MM cells (white arrowhead) (× 400, scale bar = 20 μm).

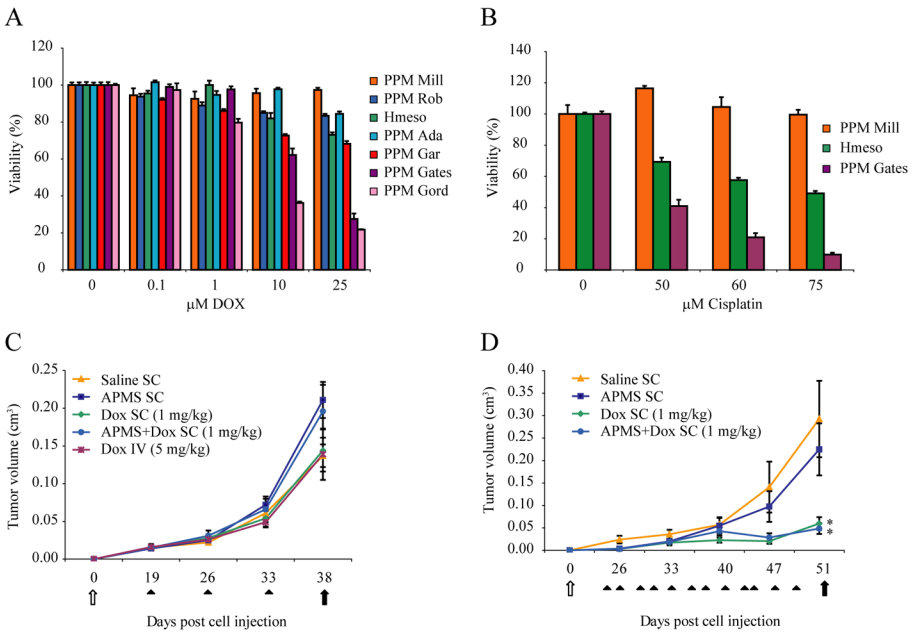

Figure 4.

Anti-tumor effect of APMS-DOX in a SC xenograft model of MM. Preliminary *in vitro* studies demonstrated human pleural MM cell lines are differentially sensitive to (**A**) DOX or (**B**) cisplatin as measured by the MTS assay when drugs are added at a range of concentrations to maintenance medium. Because the Hmeso MM line exhibited intermediate sensitivity to DOX or cisplatin and grew reproducibly when injected SC or IP in a SCID mouse xenograft model, it was used for (**C**) 1X weekly (Experiment 1) and (**D**) 3X weekly (Experiment 2) injection studies to evaluate the effects of DOX when administered systemically or loaded into APMS (APMS-DOX) on inhibition of MM growth. Systemic administration of 5 mg/kg DOX IV 3X weekly resulted in death of mice after 2 sequential doses (data not shown) * = $p<0.05$ in comparison to saline control groups. White arrows indicate time of injection of Hmeso cells (5×10^6), and black arrows indicate days at which mice were euthanized in respective experiments. Black arrowheads indicate times at which saline, APMS alone (160 mg/kg), DOX alone (1 mg/kg), and APMS-DOX (160 mg/kg APMS; 1 mg/kg DOX equivalent) were injected into mice. Each point represents the mean volume of all tumors within a particular treatment group ± SEM.

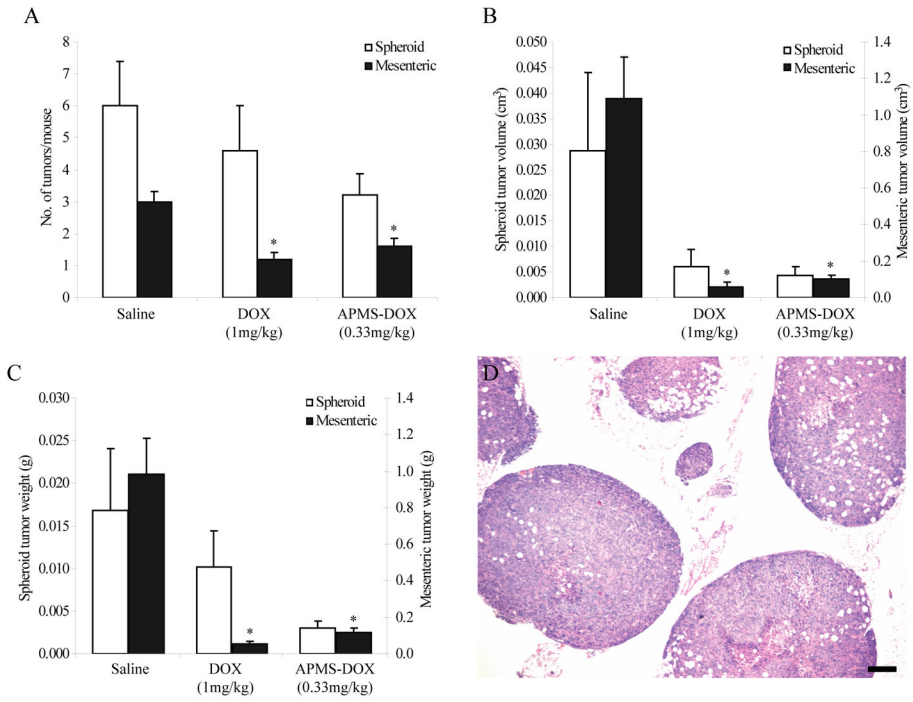

Figure 5.

Anti-tumor effect of APMS-DOX in an IP xenograft model of MM. DOX (1 mg/kg) and APMS-DOX (104 mg/kg APMS; 0.33 mg/kg DOX equivalent) administered IP 3X weekly for 1 week were equally effective in decreasing Hmeso IP mesenteric tumor (**A**) numbers, (**B**) volumes, and (**C**) weights. Trends suggest that DOX and APMS-DOX were also effective in decreasing IP spheroid tumor numbers, volumes, and weights, although statistical significance was not achieved. In (B) and (C), the left axis corresponds to spheroid tumors and the right axis corresponds to mesenteric tumors. * = $p<0.05$ in comparison to saline control group. For each mouse, total tumor weight and volume were calculated separately for spheroids and mesenteric tumors by multiplying the average tumor weight and volume by the total number of spheroid and mesenteric tumors present, respectively. Bars represent the mean value for each treatment group ± SEM of n = 5 mice/group. (**D**) Representative H&E staining of spheroids from IP xenografts indicates a biphasic MM tumor type (× 40, scale bar = 200 μm).

Table 1

Summary of *in vivo* treatment regimens following establishment of Hmeso tumors SC or IP.

Exp #	Group	# Mice/Group	Route*	Inj/Week	APMS Dose† (mg/kg)	DOX Dose‡ (mg/kg)
1	Saline§	2	SC	1	—	—
	APMS		SC	1	160	—
	DOX		SC	1	—	1
	DOX		IV	1	—	5
	APMS-DOX		SC	1	160	1
2	Saline	4	SC	3	—	—
	APMS		SC	3	160	—
	DOX		SC	3	—	1
	DOX		IV	3	—	5
	APMS-DOX		SC	3	160	1
3	Saline	5	IP	3	—	—
	DOX		IP	3	—	1
	APMS-DOX		IP	3	104	0.33

*IP - intraperitoneal; IV - intravenous; SC - subcutaneous

†160 mg/kg APMS equivalent to 3×10^8 APMS/tumor or 1.2×10^9 APMS/mouse; 104 mg/kg APMS equivalent to 7.8×10^8 APMS/mouse (assuming 25 g mouse)

‡For SC injections, each tumor injected with 6.15 μg DOX, equivalent to ~25 μg/mouse or 1 mg/kg total dose (assuming 25 g mouse)

§0.9% NaCl, pH 7.4

Note: Exp – experiment; Inj – injection